Rheo-Optics of Poly(2-hydroxyethyl methacrylate) Gels. I. Effect of Nature and Amount of Diluent

M. Ilavsky and W. Prins*

Department of Chemistry, Syracuse University, Syracuse, New York 13210.
Received March 30, 1970

ABSTRACT: Poly(2-hydroxyethyl methacrylate) networks are of practical interest because of their use as biomedical materials and of theoretical interest because their polymer chains are markedly amphiphilic in nature. Rheo-optical studies were therefore conducted at $T = 25°$ in the rubbery region on samples (concentration of cross-linker 0.065×10^{-4} mol/cm^3) swollen to equilibrium in tetrahydrofuran (THF), acetone, water, ethylene glycol, 0.5 M $Mg(ClO_4)_2$ in H_2O, 50:50 mixtures of water and THF, as well as of water and acetone. These diluents yield a range of volume degrees of swelling, q, from 1.6 to 7. Anisotropic light scattering in all cases reveals a certain amount of long-range orientation correlation over thousands of ångströms. Stress and birefringence relaxation data at various elongations ($\Lambda = L/L_0 = 1$–1.6) were found to be separable in an elongation-dependent and a time-dependent factor. The latter factor is viscoelastic in nature (changes in swelling due to the imposed strain are minor), and is governed mainly by the value of q. In THF, acetone, and water, the time dependence of the birefringence was found to differ from the time dependence of the stress. These differences find a logical explanation if one assumes that during stress relaxation there is—in addition to the normal loss of orientation proportional to the stress—a process of (re)formation of correlated regions proportional to the loss of stress. The extrapolated equilibrium stress and birefringence fit a two-parameter Mooney–Rivlin equation much better than the Gaussian one-parameter equation. The C_2^*/C_1^* ratio decreases to zero in high-swelling diluents, whereas the C_1^* term (after the normal correction for swelling) remains constant. The equilibrium stress–optical coefficient, $\Delta n/\sigma$, which is independent of Λ, depends very markedly on the refractive index of the diluent showing that form birefringence plays an important role. A detailed analysis of all equilibrium results, as well as of the time dependencies, supports the concept of some structural order exceeding that implied by a Gaussian network. This order is probably imposed by inhomogeneous cross-linking as well as by specific diluent–polymer interactions dictated by the amphiphilic nature of the polymer.

Copolymerization of 2-hydroxyethyl methacrylate (HEMA) and a small amount of ethylene glycol dimethacrylate (EGDMA) leads to cross-linked (PHEMA) polymer networks which are of practical interest because of their use as biomedical materials[1] and of theoretical interest because the constituent macromolecules are markedly amphiphilic in nature. Diluent-induced aggregation phenomena may therefore be expected, possibly leading to some local mesomorphic order of either nematic or smectic type.[2,3] The presence of cross-links and the atacticity of the chains most likely impede the development of crystallinity.

It is thus of interest to investigate the influence of the nature and amount of diluent on the structure and properties of such networks. An advantage of the PHEMA systems is that they can be prepared as visually clear gels, so that in addition to the mechanical behavior, also the photoelasticity and light scattering can be conveniently studied. One may hope to obtain in this way a closer insight into the relation between structure and mechanical behavior of polymer networks. Such a relation is, quite generally, very much needed in view of the fact that the behavior of virtually all networks deviates substantially from the behavior predicted by the commonly accepted structural model in which only the presence of randomly cross-linked, randomly coiled Gaussian polymer chains is postulated.

For a Gaussian network one has the following well-known relation[4] for the true equilibrium stress (*i.e.*, force per unit strained cross section)

$$\sigma = G_d^* q^{-1/3}[\Lambda^2 - \Lambda^{-1}(q_\Lambda/q)] \approx G^*[\Lambda^2 - \Lambda^{-1}] \quad (1)$$

In this equation, $\Lambda = L/L_0$ with L_0 the initial, swollen but unstrained length; $G_d^* = Aq_0^{-2/3}\nu^*RT$ with ν^* the number of moles of network chains per cubic centimeter of dry network; $q_0^{-2/3} = \langle r^2\rangle_d/\langle r^2\rangle_{os}$, *i.e.*, the ratio of the dry to the unstrained average chain dimensions in the swollen state; q_Λ and q are the strained and unstrained volume degrees of swelling, respectively. The constant A is a numerical factor reflecting a minor ambiguity in the various known derivations of eq 1. The approximation indicated in the right-hand side of eq 1 is justified if $q_\Lambda/q \simeq 1$, which is in fact the case in our study. Similarly one has for the birefringence

$$\Delta n = A_d^* q^{-1/3}[\Lambda^2 - \Lambda^{-1}] = A^*[\Lambda^2 - \Lambda^{-1}] \quad (2)$$

with $A_d^* = (G_d^*/RT)(2\pi/45)(\bar{n}^2 + 2)^2\bar{n}^{-1}\Delta\alpha_c$, where $\bar{n}$ is the average refractive index of the gel and $\Delta\alpha_c$ is the optical anisotropy of a chain segment. The latter may in principle contain an intrinsic as well as a form anisotropy.

In practice one finds that the equilibrium elastic data are frequenctly much better described by the two-parameter Mooney–Rivlin equation[4]

$$\sigma = (C_1^* + C_2^*/\Lambda)(\Lambda^2 - \Lambda^{-1}) \quad (3)$$

In this equation C_1^* is often, but without any theoretical justification, identified with the constant $G_d^* q^{-1/3}$ of the

(1) O. Wichterle and D. Lim, *Nature (London)*, **185**, 117 (1960).
(2) G. Friedel, *Ann. Phys.* (Paris), **18**, 273 (1922) (see also, R. S. Porter, E. M. Barrall II, and J. F. Johnson, *Accounts Chem. Res.*, **2**, 53 (1969).
(3) J. H. Gouda, K. Povodator, T. C. Warren, and W. Prins, *Polym. Lett.*, in press.
(4) See, *e.g.*, K. Dušek and W. Prins, *Fortschr. Hochpolym.-Forsch.*, **6**, 1 (1969).

Gaussian equation (1). Equation 3 has previously been found to hold for swollen PHEMA gels.[5]

The strain birefringence is often describable in terms of an analogous equation[6]

$$\Delta n = (A_1^* + A_2^*/\Lambda)(\Lambda^2 - \Lambda^{-1}) \quad (4)$$

again showing a substantial deviation from the Gaussian birefringence relation.

In the past years many attempts have been made to interpret the deviations from Gaussian behavior on a molecular basis. Dušek and Prins[4] have recently reviewed the various proposals. It was concluded that none of these proposals were as yet satisfactory but that the pursuit of the elusive relation between structure and elasticity would be a necessary and, hopefully, a rewarding enterprise. For a structure model in which the existence is postulated of randomly disposed, orientationally correlated (and thus anisotropic) rigid regions imbedded in a matrix of Gaussian chains, the following results are available[6-8]

$$C_2^* = 0.72\nu_{an}RT \quad (5)$$

$$A_2^* = 0.17[(\bar{n}^2 + 2)^2/\bar{n}]\phi_{an}\Delta\alpha_{an}$$

In these relations ν_{an} is the number of anisotropic regions per unit unstrained (swollen) volume, ϕ_{an} is the volume fraction of such regions, and $(\Delta\alpha)_{an}$ is their optical anisotropy (intrinsic + form) per unit volume. The C_2^* result is most unlikely since experimentally one finds $C_2^*/C_1^* \approx 1$; in conjunction with the tentative identification $C_1^* = G_d^* q^{-1/3}$ this would lead to the absurd result that the number of Gaussian chains would be of the same order of magnitude as the number of anisotropic regions. Although the A_2^* result may be more appropriate,[6,8] the above result may be an indication that the anisotropic regions should not be considered as being rigid.

In the process of obtaining equilibrium photoelasticity data, one often encounters an extended stress and birefringence relaxation. For several rubbers Thirion and Chasset[9] found that the stress can be factored in an elongation- and a time-dependent part

$$\sigma(\Lambda,t) = \sigma_e(\Lambda)\sigma_2(t) \quad (6)$$

If a reliable extrapolation for $\sigma_2(t)$ can be found experimentally, eq 6 provides $\sigma_e(\Lambda)$ which is the equilibrium stress to be used in eq 1 or 3; a similar argument should apply to the birefringence. In addition the experimentally obtained time dependencies, $\sigma_2(t)$ and $\Delta n_2(t)$ reflect linear viscoelastic behavior because they do not depend on Λ. We are, therefore, in a position to calculate the mechanical and optical relaxation spectra in the rubbery region, which may yield another clue as to the structure of the networks. If only Rouse-type configurational relaxation is involved, Read[10] has shown that both spectra should be identical, so that the stress–optical coefficient, $C = \Delta n/\sigma$ is independent of time.

Direct structural information can be obtained by performing light scattering on the unstrained gels. The angular dependence of the scattering can be analyzed in terms of long-range correlation functions or alternatively by reference to the model described above. Gouda[8] has most recently given general expressions for all light-scattering components arising from this model. For our present purpose we need only the result for the H_v component (H = horizontally polarized scattered, v = vertically polarized incident light; horizontal scattering plane), after extrapolation to zero scattering angle θ

$$(H_v)_{\theta=0} = (16\pi^4/15\lambda_0^4)\phi_{an}(\Delta\alpha_{an}^i)^2 V_{an} \quad (7)$$

In this equation λ_0 is the vacuum wavelength of the light; it should be noted that H_v depends only on the intrinsic anisotropy per unit volume, $\Delta\alpha_{an}^i$, of the regions and as such is independent of the refractive index of the surrounding. V_{an} is the volume of an anisotropic region. Equation 7 assumes that there is no anisotropy at all in the surrounding. If we want to include a contribution from the amorphous matrix, we have to add a term $(16\pi^4/15\lambda_0^4)(1 - \phi_{an})(\Delta\alpha_c^i)^2 V_c$ where $\Delta\alpha_c^i$ is the intrinsic anisotropy per unit volume of a chain segment in the matrix and V_c its volume. If desirable, one could also add a separate term for the intrinsic anisotropy of the cross-links.

Experimental Section

Preparation of Samples. All samples were prepared by copolymerization of 2-hydroxyethyl methacrylate and 0.065×10^{-4} mol/cm^3 of ethylene glycol dimethacrylate at 55°, using isopropyl percarbonate as initiator.[5a] After extraction with methanol and drying at 10^{-4} atm, their densities were determined by weighing pieces in air and in cyclohexane (which is a nondiluent). Samples were cut to $1 \times 5 \times 0.2$ cm^3 and swollen to equilibrium in tetrahydrofuran (THF), acetone (A), water (W), 0.5 M Mg$(ClO_4)_2$ in water (W–Mg), a 50 vol % THF–50 vol % H_2O mixture (W–THF), a 50 vol % acetone–50 vol % H_2O (W–A) mixture, and ethylene glycol (G) (see Table I). Volume and swollen density were measured by weighing in air and in the respective diluents. For the calculation of the volume degree of swelling, the dry density was adjusted to its liquid state equilibrium value by reference to known volume–temperature data of the dry polymer above and below its glass transition[5a] ($\alpha_l = 4.6 \times 10^{-4}$ deg^{-1}, $\alpha_g = 2.4 \times 10^{-4}$ deg^{-1}, $T_g = 90°$ yields $\rho_l = 1.016\rho_g$ at 20°).

Photoelasticity. The swollen strips were mounted between clamps in a rectangular glass cell containing diluent and given a certain amount of elongation. The length of the sample was measured to 0.005 cm between three reference marks on the sample from which two rather than one length L_i was read for increased accuracy. Subsequently the stress, $\sigma(\Lambda,t)$, and birefringence, $\Delta n(\Lambda,t)$, relaxations were measured over a period of several hours, with some extending over 5–8 hr, using a photoelasticity setup previously described.[6] The force was obtained from a transducer to ±1 g, and the birefringence, Δn, by measuring the optical retardation $\delta(t)$ ($= 2\pi\Delta nd/\lambda_0$, where $\lambda_0 = 5461$ Å and d is the thickness of the sample) in a de Sénarmont

(5) (a) J. Hasa and M. Ilavsky, *Collect. Czech. Chem. Commun.*, **34**, 2189 (1969); **33**, 2142 (1968); (b) J. Janaček and J. Hasa, *ibid.*, **31**, 2186 (1966); (c) J. Hasa, M. Ilavsky, and J. Janaček, First Microsymposium on Macromolecules, Prague, 1967.

(6) M. C. A. Donkersloot, J. H. Gouda, J. J. van Aartsen, and W. Prins, *Recl. Trav. Chim. Pays-Bas*, **86**, 321 (1967).

(7) M. V. Volkenstein, Yu. Ya. Gotlib, and O. B. Ptitsyn, *Vysokomol. Soedin.*, **1**, 1056 (1959).

(8) J. H. Gouda, Thesis, Delft, The Netherlands, 1969.

(9) R. Chasset and P. Thirion, Proceedings of the International Conference on Non-Crystalline Solids, North Holland Publishing Co., Amsterdam, 1965.

(10) B. E. Read, *Polymer*, **3**, 143 (1962).

TABLE I
MECHANICAL AND OPTICAL CHARACTERISTICS OF PHEMA GELS IN VARIOUS DILUENTS[a]

	Diluent						
	THF	A	W	W–Mg	W–THF	W–A	G
	q						
	1.64	1.79	1.85	3.57	5.26	6.25	6.99
10^{-} G^* (5 min)	1.53	1.38	1.35	0.61	0.62		
$10^{-6}G^*$ (1 hr)	1.38	1.26	1.20	0.59	0.60		
$10^{-6}G^*$ (∞)	1.13	0.98	0.92	0.57	0.59	0.50	0.37
$10^{-6}C_1^*$ (5 min)	0.97	0.89	0.94	0.44	0.45		
$10^{-6}C_1^*$ (1 hr)	0.89	0.77	0.77	0.43	0.43		
$10^{-6}C_1^*$ (∞)	0.62	0.62	0.64	0.41	0.40	0.46	0.37
$10^{-6}C_2^*$ (5 min)	0.80	0.63	0.60	0.24	0.20		
$10^{-6}C_2^*$ (1 hr)	0.74	0.68	0.55	0.21	0.20		
$10^{-6}C_2^*$ (∞)	0.71	0.57	0.54	0.22	0.18	0.05	0.0
C_2^*/C_1^* (5 min)	0.82	0.71	0.64	0.55	0.44		
C_2^*/C_1^* (1 hr)	0.83	0.88	0.71	0.49	0.46		
C_2^*/C_1^* (∞)	1.14	0.92	0.84	0.54	0.45	0.11	0
10^5A^* (5 min)	−1.69	0	2.40	4.88	1.52		
10^5A^* (1 hr)	−1.36	0	2.16	4.51	1.50		
10^5A^* (∞)	−0.84	0	1.78	4.36	1.47	2.27	0.21
$10^5A_1^*$ (5 min)	−1.13	0	1.70	4.16	1.00		
$10^5A_1^*$ (1 hr)	−1.11	0	1.45	3.32	0.97		
$10^5A_1^*$ (∞)	−0.68	0	1.30	3.06	0.93	1.63	0.04
$10^5A_2^*$ (5 min)	−0.65	0	0.90	1.00	0.66		
$10^5A_2^*$ (1 hr)	−0.33	0	0.85	1.63	0.60		
$10^5A_2^*$ (P)	−0.18	0	0.53	1.76	0.63	0.89	0.26
A_2^*/A_1^* (5 min)	0.58		0.54	0.24	0.66		
A_2^*/A_1^* (1 hr)	0.30		0.59	0.49	0.62		
A_2^*/A_1^* (∞)	0.26		0.41	0.58	0.68	0.55	6.5
$10^{11}\Delta n/\sigma$ (5 min)	−1.12	0	1.76	8.00	2.45		
$10^{11}\Delta n/\sigma$ (1 hr)	−1.04	0	1.80	7.74	2.50		
10^1 $\Delta n/\sigma$ (∞)	−0.70	0	1.95	7.75	2.51	4.70	0.58

[a] G^*, C_1^*, C_2^*, and σ are all in dyn/cm^2.

compensator, with the analyzer at −45° to the stretch direction (polarizer at +45°, slow direction in λ/4 plate at +45°). The transmitted intensity, measured on a photomultiplier, is then $I(t) \propto \sin^2[\delta(t)/2]$. The proportionality constant is obtained at the end of the experiment at time t' by rotating the analyzer through an angle φ so as to obtain minimum intensity on the detector. In this case $I(t') \propto \sin^2[\delta(t')/2 + \varphi(t')]$, so that $\delta(t')/2 = -\varphi(t')$ and thus the proportionality constant $I(t')/\sin^2[\delta(t')/2]$. The results are given in the figures in terms of the extinction angle $\varphi(t) = -\delta(t)/2$. The accuracy in $\varphi(t)$ is about 15 min.

Small-Angle Light Scattering. The measurements were taken on the instrument described previously,[11] equipped with a chopper and lock-in amplifier to accommodate the low levels of scattering.[8] The swollen gel plus a small amount of excess diluent were held between parallel glass windows. The H_h, V_v, and H_v components were measured at scattering angles $2° < \theta < 30°$ (the symbols v and h refer to the state of polarization of the incident light and H and V to that of the scattered light). The conversion of measured intensities to absolute Rayleigh ratios required an elaborate procedure, which has been detailed previously.[8] The refractive indices of the gels and diluents were measured on an Abbe refractometer.

Results

Force and birefringence (extinction angle) relaxation usually did not reach equilibrium within 5–8 hr, whereas any relaxation due to increased swelling under the imposed strain was found to be completed in about 2 hr (1–2% additional swelling at elongations $1 < \Lambda < 1.6$). Upon plotting $\log f(\Lambda,t)$ *vs.* $\log t$, series of parallel lines were obtained, provided the period of creep recovery was at least ten times the time of the relaxation experiment. An example is given in Figures 1 and 2. This proves that factoring $f(\Lambda,t) = f_e(\Lambda)\cdot f_2(t)$, as in eq 6, applies. For the extinction angle $\varphi(\Lambda,t)$, a similar separability into $\varphi_e(\Lambda)$ and $\varphi_2(t)$ applies.

Thirion and Chasset have shown that the time dependence for rubber vulcanizates can be represented by[9]

$$f_2(t) = 1 + (t/t_0)^{-m} \tag{8}$$

where t_0 and m are constants ($m \approx 0.12$), or

$$\log(-\mathrm{d}f(\Lambda,t)/\mathrm{d}\log t) = a - m\log t \tag{9}$$

so that $f(\Lambda,t) = f_e(\Lambda) + 10^a t^{-m}/2.3m$, which yields $f_e(\Lambda)$ and thus also $t_0^m = 10^a/2.3m\cdot f_e(\Lambda)$. Using this method first for that value of $\Lambda(=\Lambda^*)$ for which the longest relaxation experiment was performed, m, t_0, and $f_e(\Lambda^*)$ were obtained by the graphical use of eq 9. Subsequently the other $f(\Lambda,t)$ plots were shifted vertically to the line for $f(\Lambda^*,t)$ so as to get the best fit of the time dependencies. Next a new value for m and t_0 was obtained by a least squares fit of all the experimental points using f_e obtained for Λ^*. Subsequently f_e was changed repeatedly by 1 g and m and t_0 values were calculated until $\Sigma_i(f_{i,\mathrm{exp}} - f_{i,\mathrm{theor}})^2$ differed less

(11) A. E. M. Keyzers, J. J. van Aartsen, and W. Prins, *J. Appl. Phys.*, **36**, 2874 (1965).

TABLE II
MECHANICAL AND OPTICAL RELAXATION PARAMETERS OF PHEMA GELS IN VARIOUS DILUENTS

	Diluent				
	THF	A	W	W–Mg	W–THF
$t_0^{(m)}$, sec	3.4	1.5	0.81	1.3×10^{-3}	5.0×10^{-5}
$m^{(m)}$	0.170	0.180	0.147	0.172	0.176
$t_0^{(o)}$, sec	6.1×10		4.8×10^{-2}	1.3×10^{-3}	5.0×10^{-5}
$m^{(o)}$	0.174		0.156	0.172	0.176
Log a_q	0	−0.45	−0.65	−3.25	−4.50
Log $(t_0^{(m)}/t_{0r}^{(m)})$	0	−0.36	−0.62	−3.42	−4.83
$h^{(o)}/h^{(m)}$	1.63	0	0.62	1	1

than 1% from the previous step in the iteration. The m and t_0 values thus obtained are listed in Table II. These values were used for obtaining all $f_e(\Lambda)$ values. The same was done for $\varphi(\Lambda,t)$. In order to distinguish between the mechanical and optical parameters, we use the notation $m^{(m)}$, $t_0^{(m)}$, and $m^{(o)}$, $t_0^{(o)}$, respectively.

For the construction of the equilibrium stress–strain and birefringence–strain plots one needs, in addition to $f_e(\Lambda)$ and $\varphi_e(\Lambda)$, the actual cross section of the strip, S_Λ, and the best unstrained length, L_0. For the cross section we can put with 1–2% accuracy $S_\Lambda = \Lambda^{-1}S$, where S is the initial swollen cross section. To eliminate experimental error in L_0, an iterative, nonlinear, least squares method was used which allowed us not only to determine G^* (or A^*), C_1^*, and C_2^* (or A_1^* and A_2^*) but also L_0, as outlined in the Appendix. It is also shown there that in most cases the Mooney–Rivlin equations (2 and 4) represent the data much better than the Gaussian equations (1 and 3). In Figure 3 some representative Mooney–Rivlin (MR) plots are given. Using this procedure we not only determined the equilibrium MR plots but also the 5-min and 1-hr plots, as shown in Figure 3 (see also Table I).

The function $f_2(t)$, obtained from $f(\Lambda,t)/f_e(\Lambda)$, is independent of the elongation and thus represents the linear viscoelastic response of the sample [Young's modulus $E(t) \propto 3f_2(t)(C_1^* + C_2^*)$]. Table II shows that m is approximately the same for all diluents, for $f_2(t)$ as well as for $\varphi_2(t)$. The differences reside in the t_0 values. Figure 4 shows that all log $f_2(t)$ curves *vs.* log t are superimposable and closer to equilibrium the higher the degree of swelling. Thus we can utilize a shift factor $a_q = a_{q_r}(q)$ (Table II) to construct a master curve (Figure 5); THF with $q_r = 1.64$ was chosen as reference. The master curve is described very accurately by eq 8, as shown by the linearity of the plot in Figure 6, where eq 9 is plotted using t/a_q. The value $m = 0.17$ of the superimposed curve agrees well with the average of the m values listed in Table II. The value of $t_0^{(m)} = 3.40$ agrees with the value previously found for THF (Table II).

The birefringence time dependencies, although always describable in terms of m and t_0, are sometimes slower or faster than the corresponding force time dependencies or identical with them. Figure 7 illustrates the above conclusions by showing the time dependencies

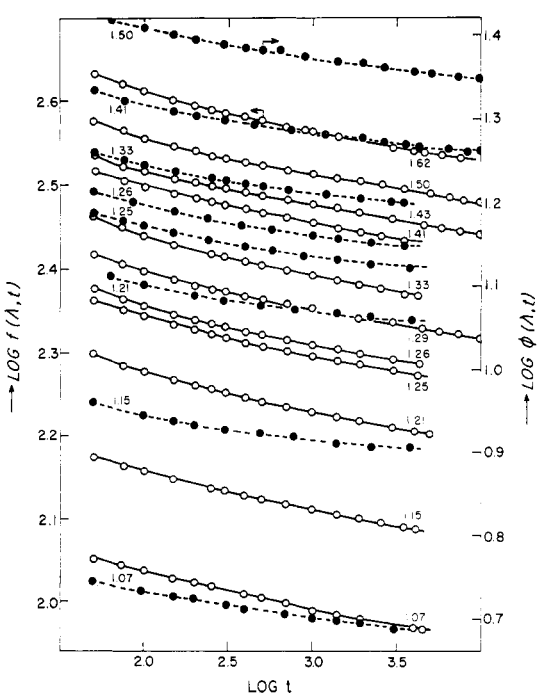

Figure 1. Experimental values of force, f in grams (○), and extinction angle, φ in degrees (●), *vs.* time (in seconds) for water swollen gel. The numbers in the graph refer to the various elongation ratios Λ.

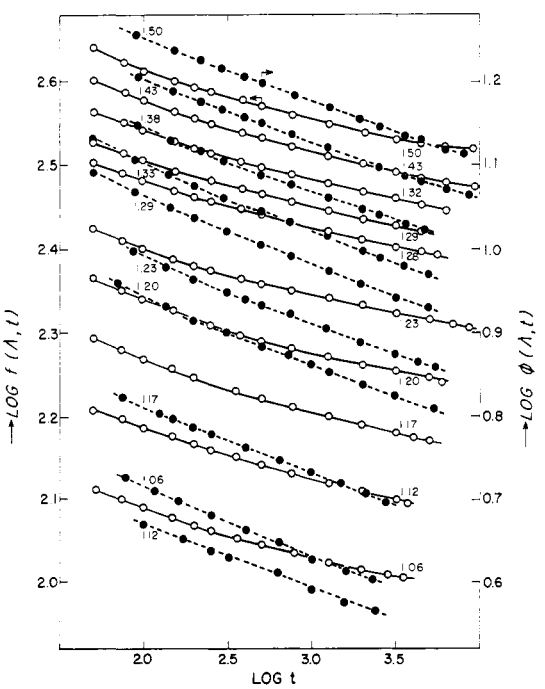

Figure 2. Experimental values of force f in grams (○) and extinction angle φ in degrees (●) *vs.* time (seconds) for THF swollen gel. The numbers in the graphs refer to the elongation ratios Λ. In this case the birefringence is negative.

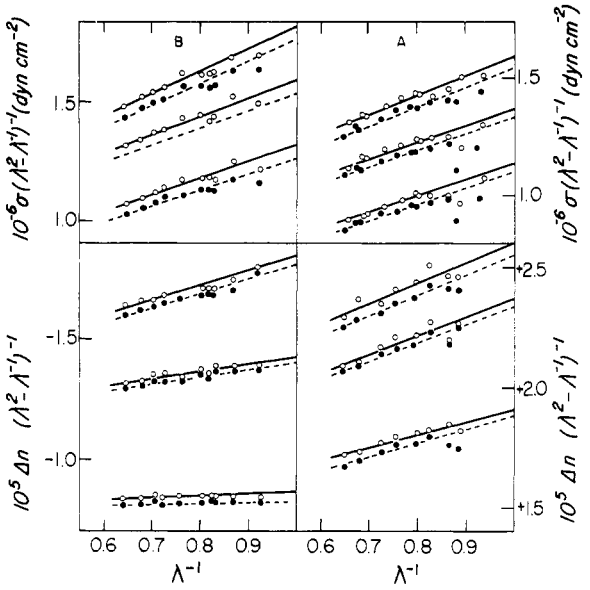

Figure 3. Mooney–Rivlin plots for stress and birefringence: A, water swollen sample; B, THF swollen sample (1, upper slopes) 5-min values, (2, middle slopes) 1-hr values, (3, lower slopes) extrapolated equilibrium values. Each MR plot is double because two different length readings were taken.

of the stress-optical coefficient, $C = \Delta n/\sigma$, in the case of water and THF. The equilibrium values (C_e) are given in Figure 8. The C_e values do not depend very much on the deformation, which indicates that roughly $C_2^*/C_1^* \approx A_2^*/A_1^*$.

The small-angle light-scattering results in all cases yielded large angular dependencies for H_h, V_v, and H_v. Figure 9 shows an example for water and ethylene glycol, including the extrapolation procedure for obtaining the zero scattering angle intensity (eq 6) by decomposing the angular dependence in three linear ranges. Table III lists the extrapolated intensities. The slopes of the straight lines, together with the associated intensities, yielded correlation distances for all gels of about 4000, 12,000, and 25,000 Å, with contributions to the total scattering of 80, 15, and 5%, respectively.

Mechanical and Optical Relaxation in the Rubbery Region. Mechanical Relaxation Spectra. The linear

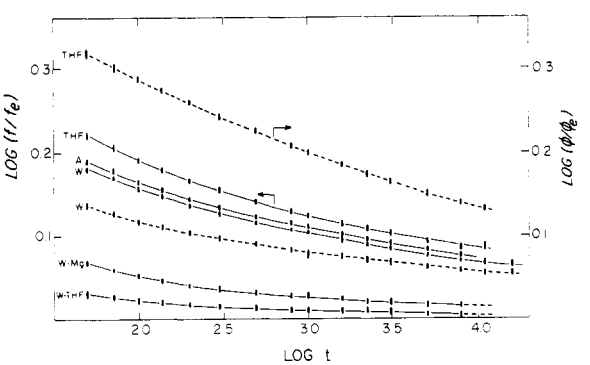

Figure 4. Time-dependent part of the stress, $f_2 = f/f_e$ (drawn lines) and extinction angle, $\varphi_2 = \varphi/\varphi_e$ (dashed lines) *vs.* time (seconds) for all gels.

TABLE III
EXTRAPOLATED SMALL-ANGLE LIGHT SCATTERING OF PHEMA GELS IN VARIOUS DILUENTS

Diluent	n_l	n_g	$(H_h)_{\theta=0} = (V_v)_{\theta=0}$, cm^{-1}	$(H_v)_{\theta=0}$, cm^{-1}
THF	1.404	1.468	5.0×10	9.0×10^{-1}
A	1.356	1.451	1.5×10^2	2.5
W	1.332	1.432	5.4×10^2	2.0
W–Mg	1.341	1.368	6.0×10	4.0×10^{-1}
W–THF	1.370	1.383	2.5×10	1.5×10^{-1}
W–A	1.356	1.367	3.0×10	9.0×10^{-2}
G	1.428	1.432	3.0	9.0×10^{-2}
D[a]		1.515	7.0	4.0×10^{-1}

[a] Dry gel measured in toluene (n_l = 1.497).

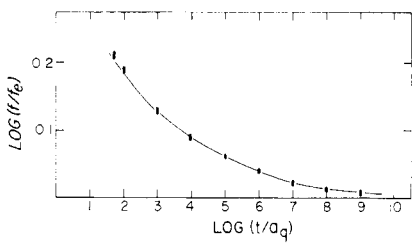

Figure 5. Superimposed time dependence of the force, f/f_e, *vs.* reduced time t/a_q. As reference the THF swollen sample has been chosen.

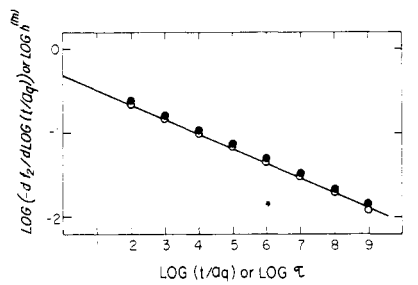

Figure 6. First approximation mechanical relaxation spectrum or test of eq 8 (○) and exact spectrum (●) *vs.* reduced time $t/a_q = \tau$.

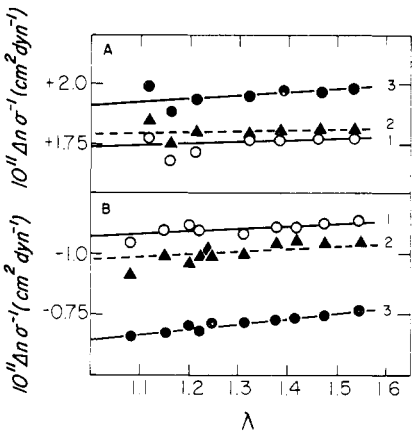

Figure 7. Stress–optical coefficients, $\Delta n/\sigma$, *vs.* the elongation Λ, for the water swollen (A) and THF swollen (B) samples: 1, experimental 5-min values; 2, experimental 1-hr values; and 3, extrapolated equilibrium values.

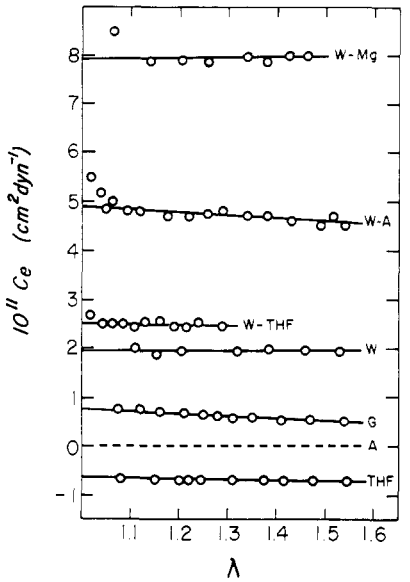

Figure 8. Extrapolated equilibrium values of the stress-optical coefficient *vs.* the elongation, for all gels.

viscoelasticity of cross-linked networks can phenomenologically be represented by

$$f_2(t) = \frac{f}{f_e} = E(t)/E_e = 1 + \int_0^{+\infty} \frac{E(\tau)e^{-t/\tau}}{E_e} d\tau = 1 + \int_{-\infty}^{+\infty} h^{(m)}(\log \tau)e^{-t/\tau} d \log \tau \quad (10)$$

where $E(t)$ and E_e are the time dependent and equilibrium (Young's) modulus, respectively, and $E(\tau)$ is the spectrum of relaxation times τ; $h^{(m)}$ is the reduced, logarithmic, mechanical relaxation spectrum. It is known that the position of $E(\tau)$ is very sensitive to the degree of swelling and a theory based on the additivity of the free volumes of diluent and polymer is available.[12] Application of this theory leads to a slightly negative free volume of our polymer. Since we are working here in a series of diluents of different chemical nature, one cannot expect this theory for the shift factor a_q to be adequate. Still the construction of the master curve (Figure 5) shows that the shift is predominantly governed by the *degree* of swelling and not by the *nature* of the diluent. Because the m values for the various diluents are essentially the same, the experimental shift factor log a_q is roughly equal to log $t_0^{(m)}/t_{0r}^{(m)}$, where $t_{0r}^{(m)}$ refers to the THF reference sample (Table II).

The master curve of Figure 5 describes the approach to equilibrium over about ten logarithmic decades of time. Since eq 8 was found to hold, a comparison with eq 10 shows that the relaxation spectrum in this (rubbery) range of time is given by

$$(t/t_0^{(m)})^{-m} = \int_{-\infty}^{+\infty} h^{(m)}(\log \tau)e^{-t/\tau} d \log \tau \quad (11)$$

or after forming the inverse Laplace transform

$$h^{(m)}(\log \tau) = \frac{2.303(t_0^{(m)})^m}{\Gamma(m)}\tau^{-m} \quad (11a)$$

where $\Gamma(m)$ is the gamma function. It may be worthwhile to point out that if we apply the so-called first approximation method of Schwarzl and Staverman[13] to eq 8 we find from our results

$$h^{(m)}(\log \tau) = 2.303m(t_0^{(m)})^m\tau^{-m}$$

which for our values of m is identical with eq 11a within the experimental error. Thus in this range of long relaxation times the first approximation method yields the exact spectrum.

Optical Relaxation Spectra. Although the m values for the optical relaxation are the same as for the mechanical relaxation, there are differences in the $t_0^{(o)}$ values leading to forward as well as backward shifts of the optical compared to the mechanical spectra (Table II). The reduced, logarithmic optical relaxation spectra follow from

$$\varphi_2(t) = \frac{\varphi}{\varphi_e} = \frac{\Delta n(t)}{\Delta n_e} = 1 + \int_{-\infty}^{+\infty} h^{(o)}e^{-t/\tau} d \log \tau \quad (12)$$

which in our case yields

$$(t/t_0^{(o)})^{-m} = \int_{-\infty}^{+\infty} h^{(o)}e^{-t/\tau} d \log \tau \quad (13)$$

The differences between $h^{(o)}$ and $h^{(m)}$ cause the stress-optical coefficients to be time dependent.

Differences between mechanical and optical spectra in the main transition have in the past[14] been attributed to an overlapping of distortional relaxations (of impor-

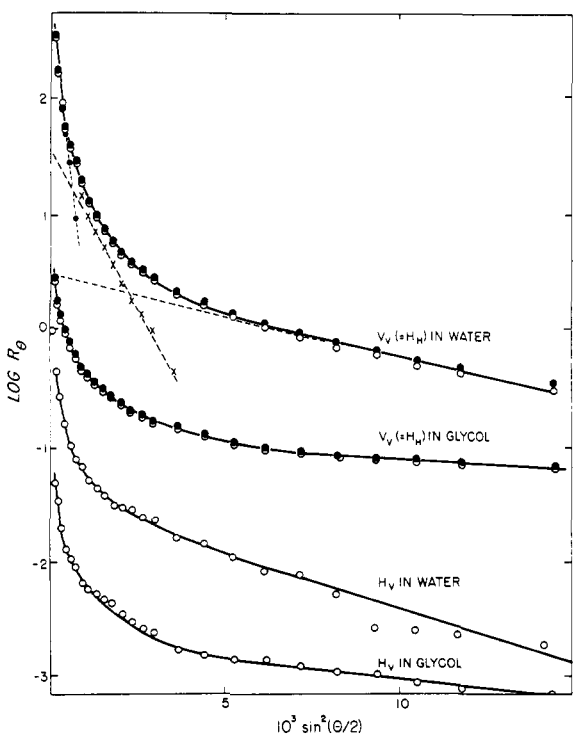

Figure 9. Rayleigh ratios (cm^{-1}) of water- and glycol-swollen gels *vs.* scattering angle.

(12) H. Fujita and A. Kishimoto, *J. Chem. Phys.*, **34**, 393 (1961).
(13) F. Schwarzl and A. J. Staverman, *Appl. Sci. Res.*, **A4**, 127 (1953).
(14) B. E. Read, *Polymer*, **5**, 1 (1964).

tance near the glassy region) and configurational relaxation processes (*e.g.*, Rouse-type spectrum with slope $-1/2$ beyond the glassy region). Since we are operating in the rubbery region far beyond the glassy region and even beyond the Rouse single molecule region of slope $-1/2$, this approach is unlikely to be of help in explaining our results. Stein[15] has developed a general phenomenological theory in terms of two distributions of relaxation times, appropriate to crystalline polymers. A connection between these distributions and the mechanical spectrum is, however, lacking.

For an explanation of the differences in spectra in the rubbery region, we recapitulate our findings once again: in water the positive birefringence decreases slower than the stress, in THF the negative birefringence decreases faster than the stress, in acetone there is no birefringence. If we postulate that concurrent with the stress relaxation we not only lose a certain amount of chain orientation (with positive or negative birefringence) but also *create* some new birefringence proportional to the amount of stress lost at any time, due to a *restructuring* or recreation of orientational correlation. the spectral differences find a straightforward explanation. Since we know from the light-scattering results (Figure 9) that in the unstressed networks such a structure exists, its re-formation after its partial or complete destruction upon initially straining the material is not such a far-fetched idea.

In order to formulate this idea in as general a way as possible we write

$$\Delta n(t) = \Delta n^{(c)}(t) + \Delta n^{(nc)}(t) = C^{(c)}\sigma(t) + C^{(nc)}(t)(\sigma(0) - \sigma(t)) + \Delta n^{(nc)}(0) \quad (14)$$

where $\Delta n^{(c)}(t)$ is the birefringence relaxation due to the normal configurational relaxation of the chains ("Rouse-type" relaxation) and $\Delta n^{(nc)}(t)$ simply denotes the nonconfigurational (possibly structural) part. The second line of eq 14 introduces the configurational and nonconfigurational stress–optical coefficients of which it is known that the first is not time dependent; since at zero time the birefringence is not solely dictated by the configurational part but also by distortional or any further structural contributions, a term for $\Delta n^{(nc)}(0)$ at zero time has to appear in eq 14. Next, we introduce

$$\sigma(t) = \sigma_e + \Delta\sigma \int_{-\infty}^{+\infty} H_\tau e^{-t/\tau}\, d\log\tau \quad (15)$$

where $\Delta\sigma = \sigma(0) - \sigma_e$, σ_e is the equilibrium stress, and H_τ is the normalized logarithmic relaxation spectrum. By comparison with eq 10, the latter is defined by

$$\int_{-\infty}^{+\infty} H_\tau\, d\log\tau \equiv (\sigma_e/\Delta\sigma)\int_{-\infty}^{+\infty} h^{(m)}\, d\log\tau = 1 \quad (16)$$

Equation 14 now transforms to

$$\Delta n(t) = C^{(c)}\sigma_e + C^{(nc)}(t)\,\Delta\sigma + \Delta n^{(nc)}(0) + (C^{(c)}\Delta\sigma - C^{(nc)}(t)\Delta\sigma)\int_{-\infty}^{+\infty} H_\tau e^{-t/\tau}\, d\log\tau \quad (17)$$

or introducing the equilibrium birefringence, Δn_e

$$\Delta n_e = C^{(c)}\sigma_e + C_e^{(nc)}\Delta\sigma + \Delta n^{(nc)}(0) \quad (18)$$

(15) R. S. Stein, S. Onogi, and D. A. Keedy, *J. Polym. Sci.*, 57, 801 (1962).

where $C_e^{(nc)}$ is the equilibrium value of the nonconfigurational stress–optical coefficient, we have

$$\varphi_2(t) = \frac{\Delta n(t)}{\Delta n_e} = \frac{C^{(c)}\sigma_e + \Delta n^{(nc)}(0)}{\Delta n_e} + \frac{C(t)^{(nc)}\Delta\sigma}{\Delta n_e} + \frac{\Delta\sigma[C^{(c)} - C^{(nc)}(t)]}{\Delta n_e}\int_{-\infty}^{+\infty} H_\tau e^{-t/\tau}\, d\log\tau \quad (19)$$

The birefringence relaxation $\varphi_2(t)$ can thus be quite generally written in terms of a constant and two functions of time. This is similar to Stein's phenomenological formulation in terms of two optical spectra. Equation 19 offers the advantage, however, of being directly related to the mechanical spectrum H_τ. In principle any time dependence of $\varphi_2(t)$ can thus be analyzed in conjunction with $f_2(t)$ data, so as to yield optical spectra for which molecular explanations may then be sought.

The experimental results show that in our case $h^{(o)} \propto h^{(m)}$ (eq 11 and 13). Upon inserting this result in eq 19 and utilizing eq 16, one has to conclude that $C^{(nc)}(t)$ must be a constant, independent of time, which is thus a special case of the more general formulation. It is at this moment that we can write $C^{(nc)}(t) = C^{(r)}$ in order to reflect its relation to a certain restructuring of the network proportional to the amount of stress lost at a given time. Equation 19 reduces to

$$\varphi_2(t) = 1 + K\int H_\tau e^{-t/\tau}\, d\log\tau \quad (20)$$

with

$$K = \Delta\sigma(C^{(c)} - C^{(r)})/\Delta n_e$$

and

$$\Delta n_e = C^{(c)}\sigma_e + [C^{(r)}\Delta\sigma + \Delta n^{(nc)}(0)] = \Delta n_e{}^{(c)} + \Delta n_e{}^{(nc)} \quad (21)$$

For the stress–optical coefficient we will get

$$C(t) = \frac{\Delta n(t)}{\sigma(t)} = C_e\frac{\left[1 + K\int_{-\infty}^{+\infty} H_\tau e^{-t/\tau}\, d\log\tau\right]}{\left[1 + \Delta\sigma\Big/\sigma_e\int_{-\infty}^{+\infty} H_\tau e^{-t/\tau}\, d\log\tau\right]} \quad (22)$$

where $C_e = \Delta n_e/\sigma_e$. Equation 22 shows that the stress–optical coefficient will be independent of time only if

$$\Delta\sigma/\sigma_e = K = \Delta\sigma(C^{(c)} - C^{(r)})/\Delta n_e \quad (23)$$

which will be fulfilled if $C^{(r)} = 0$, *i.e.*, if only configurational relaxation occurs ($C_e = C^{(c)}$), but also if $C^{(r)}$ fortuitously equals $-\Delta n^{(nc)}(0)/\sigma(0)$.[16]

(16) It is worthwhile mentioning that *cross-linked* networks according to eq 22 will show a time-*dependent* stress–optical coefficient even if the mechanical ($h^{(m)}$) and optical spectra ($h^{(o)}$) are proportional to each other (as is true in our case) whereas for *noncross-linked* systems such a proportionality leads to a time *independent* stress–optical coefficient. Again considering the case that $C^{(nc)}(t)$ is equal to a time-independent constant $C^{(r)}$, we have

$$\Delta n(t) = \Delta n^{(nc)}(0) + C^{(c)}\sigma(t) + C^{(r)}(\sigma(0) - \sigma(t))$$

Since Δn_e and σ_e are both zero in the noncross-linked case $\Delta n^{(nc)}(0) = -C^{(r)}\sigma(0)$ must always be valid. As a result

$$\Delta n(t) = \sigma(0)(C^{(c)} - C^{(r)})\int H_\tau e^{-t/\tau}\, d\log\tau$$

which shows that $C = \Delta n(t)/\sigma(t)$ will be time independent but the optical spectrum will be shifted by a factor $h^{(o)}/h^{(m)} = C^{(c)} - C^{(r)}$.

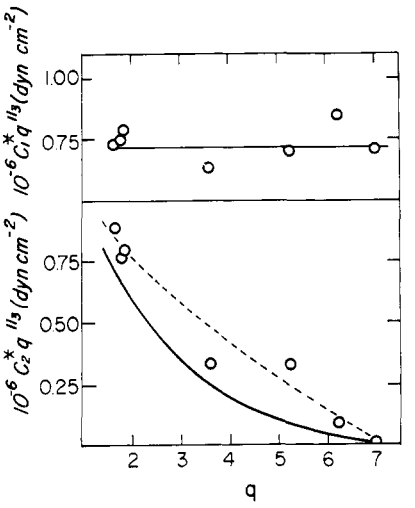

Figure 10. Reduced C_1^* and C_2^* constants *vs.* the degree of swelling q. Drawn line in C_2^* graph represents the dependence of the reduced C_2^* *vs.* the degree of swelling in ethylene glycol.[10]

Equations 10 and 12, together with the analysis resulting in eq 20, allow us to make the connection between the optical and mechanical spectra

$$h^{(o)}/h^{(m)} = \sigma_e(C^{(c)} - C^{(r)})/\Delta n_e = (t_0^{(o)}/t_0^{(m)})^{0.17} \quad (24)$$

taking the value of $m = 0.17$ for both the optical and mechanical case. H_r remains inaccessible because $h^{(m)} = (\Delta\sigma/\sigma_e)H_r$ and $\Delta\sigma$ is not experimentally available (the measurements do not extend to zero time). We now have the following three experimental results (Table II): in water, $h^{(o)}/h^{(m)} < 1, \Delta n_e > 0$; in THF, $h^{(o)}/h^{(m)} > 1, \Delta n_e < 0$; in acetone, $h^{(o)}/h^{(m)} = 0, \Delta n_e = 0$ and $C^{(c)} = C^{(r)}$. From eq 24 and 21, it then follows that

$$C^{(r)} \gtrless -(\Delta n_e - C^{(c)}\sigma_e)/\sigma_e = -\Delta n^{(nc)}(0)/\sigma(0) \quad (25)$$

indicating that the constant $C^{(r)}$, which is indicative for the restructuring during stress relaxation, is subject to the same condition in all three cases. This might be taken as an indication that the same type of restructuring occurs. Since $\Delta n_e - C^{(c)}\sigma_e = \Delta n_e^{(nc)}$ is unknown in magnitude as well as sign, we cannot determine whether $C^{(r)}$ will be positive or negative. For the other four diluents no time dependencies were found in either the stress or the birefringence so that in these cases we are unable to say whether only configurational relaxation takes place or not. Measurements at shorter time scales (dynamic measurements) would perhaps reveal the existence of nonconfigurational relaxation.[17]

Finally, some comments should be made regarding the time dependence of the parameters in eq 1–4. Table I shows the value of these constants calculated at 5 min, 1 hr, and after extrapolation to infinite time. We note that C_1^* seems to be more time dependent than C_2^*. This is contradictory to the experimentally found separability of $\sigma(\Lambda,t)$ into $\sigma_e(\Lambda)\cdot\sigma_2(t)$; insertion of this result in the MR equation shows that $C_2^*(t)$ and $C_1^*(t)$ should have the same time dependence. We have to keep in mind that the data are forced to fit the phenomenological MR equation and moreover that the accuracy in C_2^* is not very high. A similar statement applies to the optical constants A_1^* and A_2^*.

Although it is likely that C_2^*/C_1^* and A_2^*/A_1^* are related to the deviations from Gaussian behavior, we have as yet been unable to find a straightforward connection with the restructuring process outlined earlier.

Mechanical and Optical Equilibrium Behavior. There is no doubt that the equilibrium stress in most diluents is described much better by the Mooney–Rivlin equation (3) than by the Gaussian equation (1) (compare Figure 3 and Table I). Figure 10 shows that C_1^*—if corrected for swelling by the Gaussian factor $q^{1/3}$ (see eq 2)—is essentially constant for all diluents, whereas C_2^*, similarly plotted, decreases to zero in the high swelling diluents. The light-scattering intensities, collected in Table III as Rayleigh ratios, similarly decrease with increased swelling. The decrease in H_v far exceeds what we would calculate from eq 7 assuming just a decrease in the volume fraction of anisotropic regions, ϕ_{an}, but keeping the intrinsic anisotropy per region unchanged. This suggests that the anisotropic regions themselves change with the diluent, although the range of the orientation correlation is not critically affected by the swelling, presumably because of the presence of cross-links. It thus seems logical to connect C_2^* or the ratio C_2^*/C_1^* with deviations from the Gaussian network structure. The model of rigid anisotropic regions embedded in a Gaussian matrix (eq 5), however, leads to physically impossible values for the volume fraction of such regions. One way of getting around this difficulty is stipulating that only a very minor fraction of the stress is borne by these regions. This concept is in agreement with the explanation of the time-dependent behavior which necessitated the introduction of a restructuring during stress relaxation (see above). Such restructuring implies the breaking up of anisotropic regions and their re-formation under stress. In other words, the regions are not rigid but rather loosely held, and cannot carry much of the load.

The optical behavior can shed some further light on the nature of the gel structure. Contrary to C_1^* and C_2^*, the A_1^* and A_2^* constants of eq 4 are not governed by the degree of swelling, so that not even A_1^* or $A_1^* \cdot q^{1/3}$ is relatable to the Gaussian result of eq 2. Instead, both constants decrease markedly with the refractive index of the gels, and become negative above $n_g = 1.45$ (dry gel $n_g = 1.515$). In principle this might be taken as an indication that there are specific diluent effects leading to widely different intrinsic anisotropies of either the chain segments or correlated anisotropic regions. A comparison with the H_v light-scattering component which measures exclusively the intrinsic anisotropy shows that this cannot be so: there is no correlation between A_1^*, A_2^*, and H_v. The conclusion must therefore be that in the A_1^*,A_2^* behavior the form birefringence plays an important role.

Because of this finding it is not permissible to compute ν_{an} and $V_{an}\Delta\alpha_{an}$ from eq 5 and 7, as has in fact been done in recent contributions from this laboratory.[6,18] On the other hand, the existence of large form effects sup-

(17) Such measurements are planned in this laboratory.

(18) R. Blokland and W. Prins, *J. Polym. Sci., Part A-2*, 7, 1595 (1969).

ports the contention that PHEMA gels are structured in some fashion. This can be seen as follows. In all gels investigated by us the polymer concentration is sufficiently high to eliminate the macroform anisotropy of Gaussian chains because this form effect only exists if there are unequal segment densities in the gel. Furthermore, the microform anisotropy of the individual chain segments as discussed by Tsvetkov and Grishchenko[19] cannot adequately explain our results. This can be seen by plotting the equilibrium stress-optical coefficient C_e (see Table I) *vs.* the refractive index of the gels (see Table III). In view of the discussion below, we have plotted in Figure 11 the values of the segmental anisotropy which one calculates from C_e, assuming the validity of eq 1 and 2

$$\Delta\alpha_c = (4\pi k\tau/2\pi)(\bar{n}^2 + 2)^{-2}\bar{n}\Delta n_e/\sigma_e \qquad (26)$$

It is seen that $\Delta\alpha_c$ in water is four times larger than in ethylene glycol, whereas the swelling in the latter diluent is 3.5 times larger than in water. The refractive indices of both gels being the same, one would expect the microform anisotropy to be much larger at the higher degree of swelling.[19] An analogous case is provided by the segmental anisotropies of the samples in aqueous $Mg(ClO_4)_2$ solution and in the acetone–water mixture. One is thus forced to conclude that the networks do not at all behave optically as Gaussian networks would.

The light-scattering results in water and ethylene glycol are in agreement with the above conclusion. Table III shows that the H_v scattering (and thus the intrinsic anisotropy, see eq 7) is much larger in water than in ethylene glycol. In a previous communication[3] this large difference has been connected with the presence and absence, respectively, of local mesomorphic ordering.[20]

The same reasoning can be applied to the $Mg(ClO_4)_2$ and acetone–water case in Table III and Figure 11.

The segmental anisotropy, $\Delta\alpha_c$, plotted in Figure 11 *vs.* the refractive index of the gels, ranges from 21×10^{-25} to -2×10^{-25} cm^3. Data of Gent[21] on *cis*- and *trans*-polyisoprene networks gave $\Delta\alpha_c$ values ranging from 4 to 6 and 6 to 10×10^{-24} cm^3, respectively, over degrees of swelling very similar to ours. Gent ascribes his optical anomaly in terms of geometric packing of the diluent around the chain segments. The magnitude of our optical anomalies are such as to make this explanation for our case not very likely. Since microform anisotropy has already been excluded earlier, we feel justified in interpreting our results once again in terms of structuring, leading to sizable correlated regions exhibiting intrinsic as well as form anisotropy.

Conclusions

The detailed analysis of all rheo-optical results as presented above show that the PHEMA gels cannot be regarded as cross-linked collections of randomly coiling Gaussian chains. The light scattering shows that in all diluents orientational correlation between chains or portions of chains extends over long distances of the order of 5000 Å. These correlated regions should, however, not be considered as rigid rods in an amorphous Gaussian matrix. Such an assumption leads to a contradiction for the C_2* Mooney–Rivlin constant, and runs counter to the observed differences in mechanical and optical relaxation spectra. The spectral differences can be described by two processes, *viz.*, a normal Rouse-type configurational relaxation of the chains proportional to the stress $\sigma(t)$ and an intermolecular structural reorganization proportional to the loss of stress $\sigma(0) - \sigma(t)$. This composite time-dependent behavior suggests that the original interchain correlation, which exists in the unstressed state, is (partially) destroyed upon imposing a deformation and is replaced during stress relaxation by oriented regions of interchain correlation. The very strong dependence of the equilibrium stress-optical coefficient on the refractive index of the diluent again supports the contention that there are oriented regions of correlated chains in addition to normal Gaussian chains. The observed large form birefringence effects show that these regions—at least in the stressed state—are nonspherical.

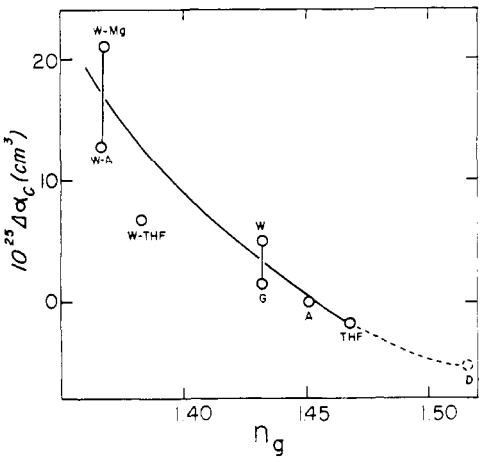

Figure 11. Segmental anisotropy, $\Delta\alpha_c$, *vs.* the refractive index n_g for all gels.

The reasons for these pronounced structural, mechanical, and optical deviations from the predictions of the common Gaussian theory, in the case of water, THF, and acetone, may well reside in specific diluent–polymer interactions. These interactions could be specific solvation of the side groups and/or withdrawal of the hydrocarbon polymer backbone from diluent contact. Thus it appears that the amphiphilic nature of the polymer chains could be responsible for the observed behavior. In a previous communication on the behavior in water, the regions of interchain correlation were thought to be regions of mesomorphic order. The data in acetone and THF point to a similar explanation.

In three diluents (50% acetone–50% water, 50% THF–50% water, 0.5 *M* $Mg(ClO_4)_2$–water), the swelling is much higher and there are no observable differences in optical and mechanical relaxation spectra. This

(19) V. N. Tsvetkov and A. E. Grishchenko, *J. Polym. Sci., Part C*, **16**, 3195 (1967).

(20) Previously the light-scattering intensities in water have been found to be about ten times lower[3,8] than our values. This discrepancy is most likely due to a higher level of interface scattering in our case due to the preparation of the samples in Teflon rather than glass molds.

(21) A. N. Gent, *Macromolecules*, 2, 262 (1969).

does not indicate that any structure is absent in these diluents, but rather that the gels very rapidly approach their equilibrium state. A strong refractive index dependence of the stress-optical coefficient as well as a Mooney–Rivlin C_2^* term remain in evidence. Only in ethylene glycol with a degree of swelling of 7 are the deviations from Gaussian behavior essentially zero. Even in this case, however, an angular dependence of the light scattering is observed. It seems likely that inhomogeneous cross-linking is responsible for this. The gels were all prepared by copolymerization in water, which is a semiincompatible diluent for the polymer, so that the conditions for inhomogeneous cross-linking[4] are very favorable.

It seems justified, therefore, to conclude finally that inhomogeneous cross-linking imposes some deviations from Gaussian behavior, and that—depending on the diluent medium—such deviations can be reinforced by a certain amount of mesomorphic ordering due to the amphiphilic nature of the polymer chain.

The structural information revealed by the optical behavior is not clearly reflected in the mechanical behavior. Both the time dependent and the equilibrium mechanical response seem to be mainly governed by the degree of swelling.

Acknowledgments. The financial support of the Syracuse University Research Institute is gratefully acknowledged. M. I. expresses his gratitude to the Institute of Macromolecular Chemistry, Czechoslovak Academy of Sciences, for granting a leave of absence. The assistance of J. Hasa, Prague, in the initial preparative work and in the three-parameter least squares procedure is gratefully remembered by the authors.

Appendix

The parameters C_1^*, C_2^*, and L_0 in eq 3 and A_1^*, A_2^*, L_0 in eq 4 are determined by a nonlinear least squares method because L_0 is difficult to obtain experimentally (especially in swollen gels) and because the various force, angle, and length values should be properly weighted in eq 3 and 4.

We require, quite generally for n observations of x_i and y_i with experimental random errors of $\pm m_{xi}$ and $\pm m_{yi}$, that a functional dependence F_i holds such that[22]

$$F_i = F_i(A, B, C, x_i + v_{xi}, y_i + v_{yi}) = 0 \quad \text{(A-1)}$$

where $i = 1, 2, \ldots$. Expanding around A_0, B_0, C_0, retaining only the first-order terms

$$F_i = F_i(A_0, B_0, C_0, x_i, y_i) + (\partial F_i/\partial A)\mathrm{d}A + (\partial F_i/\partial B)\mathrm{d}B + (\partial F_i/\partial C)\mathrm{d}C + (\partial F_i/\partial x)v_{xi} + (\partial F_i/\partial y)v_{yi} = \Phi_i + a_i\mathrm{d}A + b_i\mathrm{d}B + c_i\mathrm{d}C + (F_{xi}v_{xi} + F_{yi}v_{yi}) = 0 \quad \text{(A-2)}$$

Introducing $-v_i = (F_{xi}v_{xi} + F_{yi}v_{yi})$ we have

$$v_i = a_i\mathrm{d}A + b_i\mathrm{d}B + c_i\mathrm{d}C + \Phi_i \quad \text{(A-3)}$$

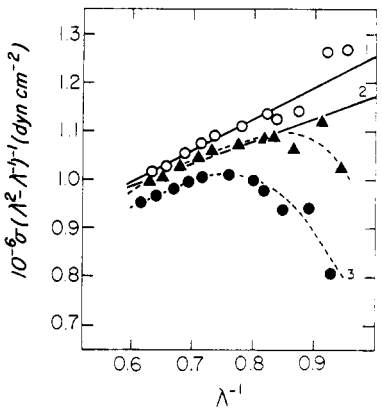

Figure 12. Computer-generated Mooney–Rivlin plots: 1, last iteration with $L_0 = 2.351$ cm; 2, first step with $L_0 = 2.328$ cm (evaluated from the first four f_i, L_i values); 3, forced fit of the Gaussian equation (A-7) with $L_0 = 2.285$ obtained by plotting $f_iL_i^2$ vs. L_i^3.

The statistical weights p_i for the deviations v_i are determined by[22]

$$p_i = (F_{xi}^2m_{xi}^2 + F_{yi}^2m_{yi}^2)^{-1} \quad \text{(A-4)}$$

in which it is assumed that the experimental errors are randomly distributed. Values for $\mathrm{d}A$, $\mathrm{d}B$, and $\mathrm{d}C$ follow from

$$\sum_{i=1}^{n} p_iv_iv_i = [\mathrm{pvv}] = \min \quad \text{(A-5)}$$

The standard error of the estimate m_0 is $\{[\mathrm{pvv}]/(n-k)\}^{1/2}$, where k is the number of constants to be determined.

For the specific case of eq 3, we have $A = C_1^*$, $B = C_2^*$, $C = L_0$, $x_i = f_i$, $y_i = L_i$, and S as initial swollen cross-section ($S_\Lambda = S\Lambda^{-1}$)

$$F_i = f_iL_i^2L_0/[L_i^3 - L_0^3]S - C_1^* - C_2^*L_0/L_i \quad \text{(A-6)}$$

and

$$\Phi_i = F_i(C_1^{*0}, C_2^{*0}, L_0^0, f_i, L_i)$$

with experimental random errors of $m_{xi} = m_f = 2$ g and $m_{yi} = m_L = 0.005$ cm.

By plotting the first three measured points at low elongation, and assuming the validity of eq 1, initial values for L_0^0 and G^{*0} were obtained. Using this L_0^0, we obtain C_1^{*0} and C_2^{*0} by the general procedure with weight factors p_i appropriate to the case that $C_1^* = G^{*0}$ and $C_2^* = 0$. Subsequently corrections $\mathrm{d}C_1^{*0}$, $\mathrm{d}C_2^{*0}$, and $\mathrm{d}L_0^0$ as well as the value of m_0^0 are calculated. The new values $C_1^{*0} + \mathrm{d}C_1^{*0}$, etc, were then introduced in eq A-6 and the whole procedure was iterated until $m_0^{(s-1)} - m_0^{(s)} < 0.01m_0^{(s-1)}$. The same procedure was used for fitting the data to eq 1 ($A = G^*$, $B = L_0$, $C = 0$, $x_i = f_i$, $y_i = L_i$)

(22) W. E. Deming, "Statistical Adjustment of Data," Wiley, New York, N. Y., 1943.

$$F_i = f_i L_i^2 L_0/s - G^* L_i^3 + G^* L_0^3$$
$$\Phi_i = F_i(G^{*0}, L_0^0, f_i, L_i) \quad \text{(A-7)}$$

For the birefringence data, procedures exactly analogous to A-6 and A-7 were followed, based on eq 4 and 2

$$F_i = \lambda_0 L_i^{3/2} L_0^{3/2} \varphi_i/(180\ \mathrm{d}(L_i^3 - L_0^3)) - A_1^* - A_2^* L_0/L_i = 0 \quad \text{(A-6a)}$$

and

$$F_i = \lambda_0 L_i^{3/2} L_0^{3/2} \varphi_i/(180\ \mathrm{d}) - A^* L_i^3 + A^* L_0^3 \quad \text{(A-7a)}$$

with $m_{xi} = m_\varphi = 15$ min, $m_{yi} = m_L = 0.005$ cm.

In all cases the iteration converges in about two to three steps for eq A-7 and four to five steps for eq A-6. In most cases (except in ethylene glycol as diluent), the two-parameter Mooney–Rivlin-type equations (A-6) describe the results better than the Gaussian-type equations (A-7), as can be seen from Figure 12. It should be noted that the best values for L_0 according to (A-7) and (A-6) do not differ more than the experimental error in L_i. The value of C_2^* is, however, very sensitive to the value of L_0 used. For $\Lambda < 1.5$ typical uncertainties in the final constants are G^* ±5%, C_1^* ±10%, and C_2^* ±20%.

The procedure outlined in this Appendix represents the best possible way of treating the data; by means of eq A-4 the various measured quantities are given proper statistical weight, *i.e.*, $f_i L_i$ values close to L_0 are weighted less than those far away from L_0, in the case of fitting to eq A-6 (for $1 < \Lambda < 1.5$, p_i varies thousandfold). For eq A-7 the statistical weights do not vary very much (for $1 < \Lambda < 1.5$, p_i varies less than twofold in opposite directions).

Rheo-Optics of Poly(2-hydroxyethyl methacrylate) Gels. II. Effect of Cross-Linking Density and Stage of Dilution during Network Formation

M. Ilavsky and W. Prins*

Department of Chemistry, Syracuse University, Syracuse, New York 13210.
Received March 30, 1970

ABSTRACT: In order to study the structure of poly(2-hydroxyethyl methacrylate) networks in water, a series of hydrogels was prepared in which the stage of dilution during copolymerization was varied (concentration of cross-linker c 0.065 × 10^{-4} mol/cm³, 0, 20, 40, 46.5, and 47% H_2O) as well as a series in which the cross-linker concentration was varied (0% water, c 0.086–2.06 10^{-4} mol/cm³). Rheo-optical studies were conducted on samples swollen to equilibrium in water at $T = 25°$ in the rubbery region. The anisotropic light scattering increases with c and decreases with the per cent H_2O during network formation; in all cases a certain amount of long-range orientation correlation exists over thousands of ångströms. Stress and birefringence relaxation data at various elongations (Λ = 1–1.6) were found to be separable in an elongation- and time-dependent factor. The viscoelastic nature of the stress–time dependence allowed the construction of a superposed curve using an apparent molecular weight between cross-links as reduction variable ($M_{app} = RTq^{-1/3}\rho_d/(C_1^* + C_2^*)$ where ρ_d = density of the dry network). The time dependence of the birefringence was found to be slower than that of the stress, with the difference between them vanishing at $M_{app} \leq 10{,}000$ g/mol. The extrapolated equilibrium stress and birefringence fit a Mooney–Rivlin representation better than a Gaussian. The C_2^*/C_1^* ratio (even after Gaussian correction to the dry state) increases with the per cent H_2O during network formation (C_2^* is about constant), but decreases rapidly with increasing c and vanishes at $M_{app} \leq 10{,}000$. The equilibrium stress–optical coefficient, which is essentially independent of Λ, rapidly decreases about ninefold with decreasing M_{app}. Upon analysis, all the above results fit the picture of a structured network as outlined in a previous paper. Because of the amphiphilic nature of the polymer, specific interaction with water may well lead to a certain type of mesomorphic ordering in the network.

Poly(2-hydroxyethyl methacrylate) networks swollen in aqueous media are currently in use as biomedical materials.[1] The structure of such PHEMA hydrogels depends very markedly on the stage of dilution during cross-linking. Visually clear gels are obtained if the water content during network formation is less than about 45 wt %. Above this critical dilution turbid gels and eventually white spongy materials are formed. The turbidity above the critical dilution is caused by the poor compatibility of the polymer with water. Cross-linked gels prepared by copolymerization below the critical dilution all swell to about 45% water—virtually independent of the cross-linking density—when they are submerged in pure water. A normal dependence of the swelling upon the cross-linking density is found[2] when one employs a good diluent as, for example, ethylene glycol.

It has been argued in previous communications[3,4] that especially in water, but also in other hydrogen-bonding diluents,[4] a certain amount of diluent-induced ordering may exist. It seems quite conceivable that

(1) O. Wichterle and D. Lim, *Nature (London)*, **185**, 117 (1960).

(2) J. Hasa and M. Ilavsky, *Collect. Czech. Chem. Commun.*, **34**, 2189 (1969).

(3) J. H. Gouda, K. Povodator, T. C. Warren, and W. Prins, *Polym. Lett.*, in press.

(4) M. Ilavsky and W. Prins, *Macromolecules*, **3**, 415 (1970).